Wireless Pers Commun (2015) 83:1213–1228
DOI 10.1007/s11277-015-2446-7

Frequency-Domain Receiver Design for Transmission Through Multipath Channels with Strong Doppler Effects

Fábio Silva · Rui Dinis · Paulo Montezuma

Published online: 11 March 2015

Abstract Single-carrier modulation (SC) with frequency-domain equalization (FDE) combined with iterative (turbo) FDE schemes has excellent performance in severely time-dispersive channels, making it a promising candidate for future broadband wireless systems. To avoid significant performance degradation due to strong Doppler effects, SC-FDE schemes employ frequency-domain receivers that require an invariant channel within the block duration. In this paper we propose iterative receivers for SC-FDE schemes able to attenuate the impact of strong Doppler effects. These receivers can be considered as modified turbo equalizers implemented in the frequency-domain, which are able to compensate the Doppler effects associated to different groups of multipath components while performing the equalization operation. The performance results show that the proposed receivers have excellent performance, even in the presence of significant Doppler spread between the different groups of multipath components. Therefore, our receivers are suitable for SC-FDE scheme based broadband transmission in the presence of fast-varying channels.

Keywords Strong Doppler effects · SC-FDE modulation · Fast-varying channels · Frequency-domain equalization · Iterative (turbo) FDE schemes · IB-DFE

1 Introduction

The tremendous growth of mobile internet and wireless multimedia communications, accompanied by the advances in micro-electronic circuits, motivated the rapid development

F. Silva (✉) · R. Dinis
Instituto de Telecomunicações, Av. Rovisco Pais 1, 1049-001 Lisbon, Portugal
e-mail: fja18393@campus.fct.unl.pt

F. Silva · R. Dinis · P. Montezuma
DEE, FCT-UNL, Monte de Caparica, 2829-516 Caparica, Portugal

P. Montezuma
UNINOVA, Campus da FCT/UNL, Monte de Caparica, 2829-516 Caparica, Portugal

of broadband wireless systems over the past decade. A very demanding challenge is to surpass the effects of the mobile radio channel, while ensuring at the same time high power and spectral efficiencies. Therefore, powerful equalization techniques like single-carrier with frequency domain equalization (SC-FDE) [1], become necessary to compensate signal distortion in time-dispersive channels.

The conventional receiver for SC-FDE schemes is a linear FDE. However, it is known that nonlinear equalizers outperform linear equalizers [2]. Iterative block decision feedback equalizer (IB-DFE) [3] is a promising iterative FDE technique for SC-FDE that was first proposed in [4] and extended to diversity scenarios [5] and layered space-time schemes [6]. These receivers can be regarded as low-complexity turbo FDE schemes [7, 8], where the channel decoder is not involved in the feedback. True turbo FDE schemes can also be designed based on the IB-DFE concept [9, 10].

In broadband wireless systems the channel's impulse response can be very long leading to very large blocks, with hundreds or even thousands of symbols. Under these conditions it can be difficult to ensure a stationary channel within the block duration, which consists a crucial requirement of conventional SC-FDE receivers. If the channel changes within the block's duration can leads to a significant performance degradation. These variations of the channel may have different origins and effects. For instance due to phase noise or residual carrier frequency offset (CFO) frequency errors may arise due to the frequency mismatch between the local oscillator at the transmitter and the local oscillator at the receiver. However, these kind of channel variations lead to simple phase variations that are relatively easy to compensate at the receiver [11, 12]. Another source of variation channel, which is not easy to compensate, is the Doppler frequency shift caused by the relative motion between the transmitter and receiver. The channel variations can become even more complex when the Doppler effects are distinct for different multipath components (e.g., when we have different departure/arrival directions relatively to the terminal movement).

In this paper we consider the use of SC-FDE schemes in channels with strong Doppler effects. We model the short term channel variations as pure almost Doppler shifts that are different for each multipath component and use this model to design frequency-domain receivers able to deal with strong Doppler effects.

The paper is organized as follows: Section 2 presents the analytical characterization adopted for modeling short term channel variations. The method for channel and CFO estimation is explained in Sect. 3. Section 4 describes the adaptative IB-DFE receivers and a set of simulation performance results is presented in Sect. 5. Section 6 resumes this paper.

2 Modeling Short-Term Channel Variations

A transmission between a mobile transmitter traveling with speed v and a fixed receiver, through a channel characterized by multipath propagation, is illustrated in Fig. 1.

Fig. 1 Doppler shift

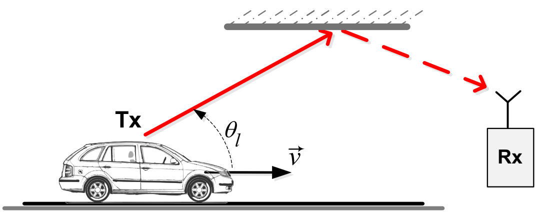

Due to the relative movement between transmitter and receiver, the received signal frequency suffers from a Doppler frequency shift, which is proportional to the speed of the transmitter and to the spatial angle between the direction of the movement and the direction of departure/arrival of the component. Therefore, the Doppler shift associated to the ith multipath component is given by

$$f_D^{(i)} = \frac{v}{c} f_c \cos(\theta_i) = f_D \cos(\theta_i), \tag{1}$$

where $f_D = vf_c/c$ represents the maximum Doppler shift, and θ_i is the angle between the velocity vector v and the arrival directions of the ith multipath component. Obviously, short term channel variations are due to the receivers motion [13].

This section presents a channel characterization appropriate to model short term channel variations. Let $h(t, t_0)$ be the channel's impulse response associated to an impulse at time t_0 given by

$$h(t, t_0) = \sum_{i \in \Phi} \alpha_i(t_0) \delta(t - \tau_i), \tag{2}$$

where Φ is the set of multipath components, $\alpha_i(t_0)$ is the complex amplitude of the ith multipath component and τ_i its delay (without loss of generality, we assume that τ_i is constant for the short-term variations that we are considering). If the channel variations are due to Doppler effects we may write

$$\alpha_i(t_0) = \alpha_i(0) e^{j2\pi f_D^{(i)} t_0} \tag{3}$$

(we will assume the specific case were the receiver and all reflecting surfaces are fixed, and the transmitter is moving as shown in Fig. 2a), and therefore (2) can be rewritten as

$$h(t, t_0) = \sum_{i \in \Phi} \alpha_i(0) e^{j2\pi f_D^{(i)} t_0} \delta(t - \tau_i). \tag{4}$$

This is a generic model in which the number of multipath components can be very high, especially when the reflective surfaces have a high roughness and/or have scattering effects. To overcome this problem, the multipath components having the same direction of arrival (i.e., following a similar path), are grouped into clusters as shown in Fig. 2b. Under this approach, the overall channel will consist on the sum of individual time shifted channels i.e.,

$$h(t, t_0) \simeq \sum_{r=1}^{N_R} \alpha_r(t_0) \delta(t - \tau_r), \tag{5}$$

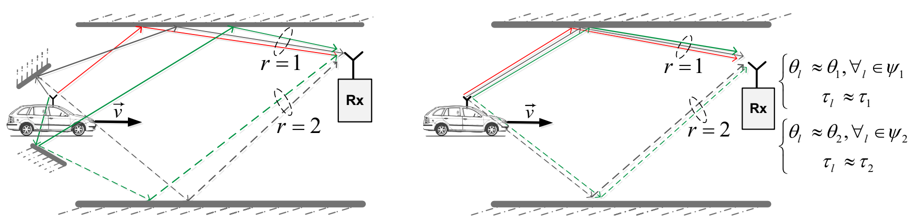

(a) **(b)**

Fig. 2 Various objects in the environment scatter the radio signal before it arrives at the receiver (**a**); Model where the elementary components at a given ray have almost the same direction of arrival (**b**) where $\alpha_r(t_0) = \sum_{i\in\Phi_r} \alpha_i(t_0)$, with $\Phi_r = \{i : \theta_i \simeq \theta^{(r)}\}$ denoting the set of elements contributions grouped in the rth multipath group. Naturally, this means that $\tau_i \approx \tau_r$, $\forall_{i\in\Phi_r}$, i.e., the contributions associated to the rth multipath group have the same delay (at least at the symbol scale).

If we assume that θ_i is uniformly distributed in $[0, 2\pi]$ and the number of components in Φ_r is $\#\Phi_r \gg 1$ (with $\#\Phi_r$ representing the number of elements in the set Φ_r), then $\alpha_r(t_0)$ can be regarded as a zero-mean complex Gaussian process with power spectral density (PSD) characterized by

$$G_{\alpha_r}(f) \propto \begin{cases} \dfrac{1}{\sqrt{1-(f/f_D)^2}}, & |f|<f_D \\ 0, & |f|>f_D, \end{cases} \tag{6}$$

which is depicted in Fig. 3a and corresponds to the so-called Jakes' Doppler spectrum. Thus, $\alpha_r(t_0)$ can be modeled as a white Gaussian noise $w(t_0)$, filtered by a filter with frequency response $H_D(f) \propto \sqrt{G_{\alpha_r}(f)}$, usually denoted "Doppler filter" [14].

It turns out that each multipath component that follows a given "macro path" is decomposed in several components that are scattered at the vicinity of the transmitter. This approximation it is acceptable for narrow band systems where the symbol duration is very high, but for broadband systems multipath components that depart/arrive with substantially different directions will have delays that are very different and therefore they should'nt be regarded as elementary components of the same ray. This means that all elementary components at a given ray should have similar direction of departure/arrival. Therefore, the Doppler filter must have a very narrow band centered in $f_D^{(r)} = f_D\cos(\theta_r)$, and consequently, short term channel's variations can be modeled as almost pure Doppler shifts that are different for each multipath group, i.e.,

$$\alpha_r(t_0) \simeq \alpha_r(0)e^{j2\pi f_D\cos(\theta_r)t_0}, \tag{7}$$

($\alpha_r(0)$ can still be modeled as a sample of a zero-mean complex Gaussian process). Under these conditions, the Doppler spectrum associated to each multipath group will have a narrow band nature, as depicted in Fig. 3b (Fig. 3c illustrates the Doppler spectrum considering a set of different multipath groups).

On the other hand, we can write the time-varying channel impulse response as

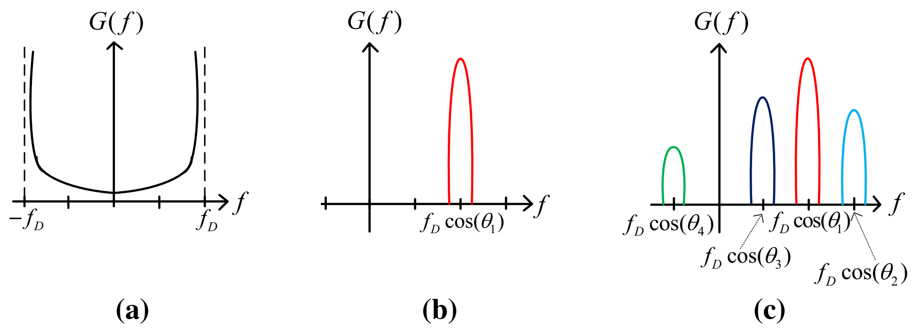

Fig. 3 Jakes power spectral density (**a**); PSD associated to the transmission of a single ray (**b**); PSD associated to the transmission of multiple rays (**c**)

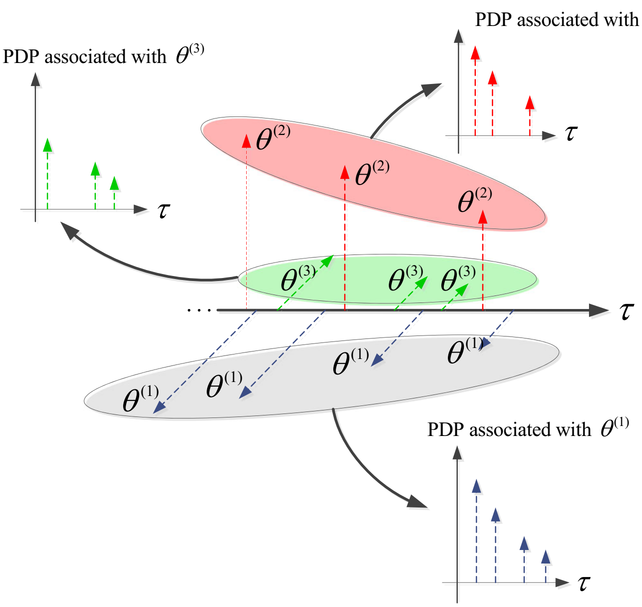

Fig. 4 Multipath components having the same direction of arrival θ are grouped into clusters

$$h(t, t_0) \simeq \sum_{r=1}^{N_R} h^{(r)}(t, 0) e^{j2\pi f_D^{(r)} t_0}, \tag{8}$$

where each individual channel $h^{(r)}(t, 0)$ is characterized by a normal power delay profile (PDP), representing the cluster of multipath components having a similar direction of arrival (although can have substantially different delays), and is given by

$$h^{(r)}(t, 0) = \sum_{i \in \Phi_r} \alpha_i(0) \delta(t - \tau_i), \tag{9}$$

where Φ_r denotes the set of all multipath components. In Fig. 4 it is shown an example of the clustering process.

In practical scenarios it might be necessary to perform a kind of quantization of the Doppler shifts.

3 Channel and CFO Estimation

3.1 Frame Structure

As already pointed out, we assume coherent receivers which require accurate channel estimates. The estimates can be obtained with the help of appropriate training sequences, or by employing efficient channel estimation methods that take advantage of the sparse nature of the equivalent channel impulse response (CIR) [15].

In the following it will be shown that the knowledge of the CIR at the beginning of the frame, together with the knowledge of the corresponding Doppler drifts, is enough to

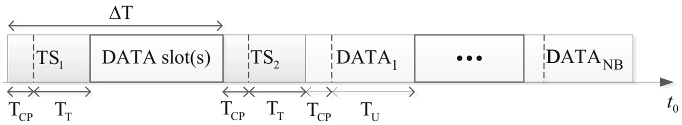

Fig. 5 Frame structure

obtain the evolution of the equivalent CIR along all the frame. The different CIRs and Doppler drifts can be obtained by employing the frame structure of Fig. 5, that starts with the transmission of two training sequences, denoted TS_1 and TS_2, respectively. Each training sequence includes a cyclic prefix with duration T_{CP}, which is longer than the duration of the overall channel impulse response (including the channel effects and the transmit and receive filters), followed by the useful part of the block with duration T_{TS}, which is appropriate for channel estimation purposes.

Between the training sequences there is a period of time ΔT, which may be used for data transmission. By employing high values of ΔT the accuracy of the estimates can be significantly improved, but it should be assured that the phase rotation within this time interval ΔT does not exceeds π.

Let us consider the first training sequence, TS_1. From the corresponding samples we can obtain the CIR, that can be eventually enhanced by using the sparse channel estimation techniques of [15], leading to the set of CIR estimates $\tilde{h}_n^{(1)}$. It can be easily shown that the corresponding estimates can be given by

$$\tilde{h}_n^{(1)} = h_n(0) + \epsilon_n^{(1)}, \tag{10}$$

where the channel estimation error $\epsilon_{n,l}$ is Gaussian-distributed, with zero-mean. Let us now consider the second training sequence,

$$\tilde{h}_n^{(2)} = h_n(\Delta T) + \epsilon_n^{(2)}, \tag{11}$$

where $h_n(\Delta T)$ denotes the channel impulse response obtained at the instant ΔT and it is simply the initial impulse response $h_n(0)$ times the corresponding phase rotation. Naturally, this is only applicable to relevant multipath components (i.e., the multipath components power must exceed a pre-defined threshold. otherwise the samples are considered as noise and ignored). Therefore, we may write (11) as

$$\tilde{h}_n^{(2)} = h_n(0) \cdot e^{j2\pi f_D \cos(\theta_n)\Delta T} + \epsilon_n^{(1)}. \tag{12}$$

For each sample we can obtain the equivalent Doppler shift from

$$f_{D,n}^{eq} = \frac{1}{2\pi\Delta T} \arg\left(\tilde{h}_n^{(2)} \cdot \tilde{h}_n^{(1)*}\right). \tag{13}$$

Using the equality $f_{D,n}^{eq} = f_{D,n} \cdot \cos(\theta_n)$, it is possible for each sample to obtain θ_n that represents the spatial angle between the direction of the movement and the direction of propagation. It should be pointed out that Independently of the delays, the samples having similar directions of arrival, are grouped together as a single channel (i.e., cluster of rays), $h_n^{(r)}$.

The information about the Doppler shift affecting the r^{th} cluster of rays, allows us to track the variations of the corresponding channel $h^{(r)}$ (provided that all rays belonging to that cluster have similar directions of departure/arrival). Therefore, results

$$\tilde{h}_n^{(r)}(\Delta T) = h_n^{(r)}(0) \cdot e^{j2\pi f_{D,n}^{(r)} \Delta T}, \tag{14}$$

where $f_{D,n}^{(r)} = f_{D,n} \cdot \cos(\theta_n^{(r)})$. It follows that it is possible to estimate the equivalent channel's impulse response for any slot, since the channel's impulse response at the instant ΔT is simply the channel's impulse response at the initial instant 0 multiplied by the phase rotation along that time interval,

$$\tilde{h}_n^{(eq)}(\Delta T) \approx \sum_{r=1}^{NR} h_n^{(r)}(0) \cdot e^{j2\pi f_{D,n}^{(r)} \Delta T}. \tag{15}$$

4 Adaptive Receivers for Signals with Strong Doppler Effects

4.1 Basic Receiver Structure

We will consider an SC-DFE scheme where the signal associated to a given block is

$$s(t) = \sum_{n=-N_G}^{N-1} s_n h_T(t - nT_S), \tag{16}$$

with T_S denoting the symbol duration, N_G denoting the number of samples at the cyclic prefix and $h_T(t)$ denoting the adopted pulse shape. The transmitted symbols s_n belong to a given alphabet Ω (i.e., a given constellation) with dimension $M = \#\Omega$ and are selected according to the corresponding bits $\beta_n^{(m)}$, $m = 1, 2, \ldots, \mu$ ($\mu = \log_2(M)$), i.e., $s_n = f(b_n^{(1)}, b_n^{(2)}, \ldots, b_n^{(\mu)})$. As with other cyclic-prefix-assisted block transmission schemes, it is assumed that the time-domain block is periodic, with period N, i.e., $s_{-n}^{(m)} = s_{N-n}^{(m)}$.

If we discard the samples associated to the cyclic prefix at the receiver then there is no interference between blocks, provided that the length of the cyclic prefix is higher than the length of the overall channel impulse response. Moreover, the linear convolution associated to the channel is equivalent to a cyclic convolution relatively to the N-length, useful part of the received block, $\{y_n; n = 0, 1, \ldots, N-1\}$. This means that the corresponding frequency-domain block (i.e., the length-N discrete fourier transform (DFT) of the block $\{y_n; n = 0, 1, \ldots, N-1\}$) is $\{Y_k; k = 0, 1, \ldots, N-1\}$, where

$$Y_k = S_k H_k + N_k, \tag{17}$$

with H_k denoting the channel frequency response for the kth subcarrier and N_k the corresponding channel noise. Clearly, the impact of a time-dispersive channel reduces to a scaling factor for each frequency.

To cope with these channel effects we can employ a linear FDE. A linear FDE is employed in conventional SC-FDE schemes to deal with channel effects. However, the performance can be substantially improved if the linear FDE scheme is replaced by an IB-DFE [3]. IB-DFE can employ "Hard decisions" or "soft decisions" in the feedback loop. A simple explanation of "IB-DFE with hard decisions" can be found in [3, 5]. References [9, 10] give a good exposition of the principles applied on "IB-DFE with soft decisions". To make this paper self-contained, the fundamental properties of lines and points of these two types of techniques are briefly described before the characterization of the proposed receivers.

For a given iteration the output samples are given by

$$\tilde{S}_k^{(i)} = F_k^{(i)} Y_k - B_k^{(i)} \hat{S}_k^{(i-1)}, \tag{18}$$

where $\{F_k^{(i)}; k = 0, 1, \ldots, N-1\}$ and $\{B_k^{(i)}; k = 0, 1, \ldots, N-1\}$ denote the feedforward and the feedback coefficients, respectively. $\{\hat{S}_k^{(i-1)}; k = 0, 1, \ldots, N-1\}$, is the DFT of the block $\{\hat{s}_n^{(i-1)}; n = 0, 1, \ldots, N-1\}$, with $\hat{s}_n^{(i-1)}$ denoting the "hard" estimate of s_n from the previous FDE iteration.

It can be shown that the optimum coefficients F_k and B_k that maximize the overall SNR in the samples $\tilde{S}_k$ are given by [3, 5]

$$F_k^{(i)} = \frac{\kappa H_k^*}{\alpha + (1 - (\rho^{(i-1)})^2)|H_k|^2}, \tag{19}$$

and

$$B_k^{(i)} = \rho^{(i-1)} \left(F_k^{(i)} H_k - 1 \right), \tag{20}$$

respectively, where

$$\alpha = E\left[|N_k^{(\ell)}|^2 \right] / E\left[|S_k|^2 \right] \tag{21}$$

and κ is selected so as to ensure that

$$\sum_{k=0}^{N-1} F_k H_k / N = 1. \tag{22}$$

The correlation coefficient $\rho^{(i-1)}$, which can be regarded as the blockwise reliability of the decisions used in the feedback loop (from the previous iteration), is given by

$$\rho^{(i-1)} = \frac{E[\hat{s}_n^{(i-1)} s_n^*]}{E[|s_n|^2]} = \frac{E[\hat{S}_k^{(i-1)} S_k^*]}{E[|S_k|^2]}. \tag{23}$$

4.2 IB-DFE with Soft Decisions

The IB-DFE described previously is usually denoted as "IB-DFE with hard decisions", although "IB-DFE with blockwise soft decisions" would probably be more adequate, as we will see in the following. In fact, (18) could be written as

$$\tilde{S}_k^{(i)} = F_k^{(i)} Y_k - B_k^{'(i)} \overline{S}_k^{Block(i-1)}, \tag{24}$$

with $\rho^{(i)} B_k^{'(i)} = B_k^{(i)}$ and $\overline{S}_k^{Block(i-1)}$ denoting the average of the block of overall time-domain chips associated to a given iteration, given by $\overline{S}_k^{Block(i-1)} = \rho^{(i-1)} \hat{S}_k^{(i-1)}$ (as mentioned above, ρ can be regarded as the blockwise reliability of the estimates $\{\hat{S}_k; n = 0, 1, \ldots, M-1\}$).

To improve the performances, we could replace the "blockwise averages" by "symbol averages", leading to what is usually denoted as "IB-DFE with soft decisions" [9, 10]. A simply way of achieving this is to replace the feedback input $\{\overline{S}_k^{Block}; k = 0, 1, \ldots, N-1\}$

by $\{\overline{S}_k^{Symbol} = \overline{S}_k; k = 0, 1, \ldots, N-1\}$ = DFT $\{\overline{s}_n^{Symbol}; n = 0, 1, \ldots, N-1\}$, with $\overline{s}_n^{Symbol}$ denoting the average symbol values conditioned to the FDE output of the previous iteration $\tilde{s}_n$, with $\{\tilde{s}_n =; n = 0, 1, \ldots, N-1\}$ denoting the IDFT of the frequency-domain block $\{\overline{S}_k; k = 0, 1, \ldots, N-1\}$. To simplify the notation, we will use $\overline{s}_n$ (and $\overline{S}_k$) instead of $\overline{s}_n^{Symbol}$ (and $\overline{S}_k^{Symbol}$) in the remaining of the paper.

For normalized QPSK constellations (i.e., $s_n = \pm 1 \pm j$) with Gray mapping it is easy to show that [10]

$$\begin{aligned} \overline{s}_n^{(i)} &= \tanh\left(\frac{L_n^{I(i)}}{2}\right) + j \tanh\left(\frac{L_n^{Q(i)}}{2}\right) \\ &= \rho_n^{I(i)} \hat{s}_n^{I(i)} + j \rho_n^{Q(i)} \hat{s}_n^{Q(i)}, \end{aligned} \tag{25}$$

with the LLRs (LogLikelihood Ratios) of the “in-phase bit” and the “quadrature bit”, associated to $s_n^I = \operatorname{Re}\{s_n\}$ and $s_n^Q = \operatorname{Im}\{s_n\}$, respectively, given by

$$L_n^{I(i)} = \frac{2}{\sigma_i^2} \tilde{s}_n^{I(i)} \tag{26}$$

and

$$L_n^{Q(i)} = \frac{2}{\sigma_i^2} \tilde{s}_n^{Q(i)}, \tag{27}$$

respectively, with

$$\sigma_i^2 = \frac{1}{2} E[|s_n - \tilde{s}_n^{(i)}|^2] \approx \frac{1}{2N} \sum_{n=0}^{N-1} |\hat{s}_n^{(i)} - \tilde{s}_n^{(i)}|^2. \tag{28}$$

The hard decisions $\hat{s}_n^{I(i)} = \pm 1$ and $\hat{s}_n^{Q(i)} = \pm 1$ are defined according to the signs of $L_n^{I(i)}$ and $L_n^{Q(i)}$, respectively and $\rho_n^{I(i)}$ and $\rho_n^{Q(i)}$ can be regarded as the reliabilities associated to the “in-phase” and “quadrature” bits of the nth symbol, given by

$$\rho_n^{I(i)} = E[s_n^I \hat{s}_n^{I(i)}] / E[|s_n^I|^2] = \tanh\left(|L_n^{I(i)}|/2\right) \tag{29}$$

and

$$\rho_n^{I(i)} = E[s_n^Q \hat{s}_n^{Q(i)}] / E[|s_n^Q|^2] = \tanh\left(|L_n^{Q(i)}|/2\right) \tag{30}$$

(for the first iteration, $\rho_n^I = \rho_n^Q = 0$ and $\overline{s}_n = 0$).

The feedforward coefficients are still obtained from (19), with the blockwise reliability given by

$$\rho^{(i)} = \frac{1}{2N} \sum_{n=0}^{N-1} (\rho_n^{I(i)} + \rho_n^{Q(i)}). \tag{31}$$

Therefore, the receiver with “blockwise reliabilities” (hard decisions), and the receiver with “symbol reliabilities” (soft decisions), employ the same feedforward coefficients; however, in the first the feedback loop uses the “hard-decisions” on each data block, weighted by a common reliability factor, while in the second the reliability factor changes from bit to bit.

4.3 Proposed Receiver Structures

Let us now consider a SC-FDE based transmission through a multipath channel with strong Doppler effects. We assume that each cluster of rays is associated with a different frequency drift due to Doppler effects, and we present two methods to compensate these effects at the receiver side. Under these conditions, each sample is affected by a different frequency drift. For a SC-FDE system the frequency drift induces a rotation in the constellation that grows linearly along the block. Without loss of generality, we assume a null phase rotation at the first sample $n = 0$.

In [12], a estimation and compensation technique of the phase rotation associated to the frequency drift is proposed for a conventional cellular system in a slowly varying scenario. Nevertheless, the multipath propagation causes time dispersion, and multiple sets of rays received with different delays are added in the receiver. Therefore, in time domain the received equivalent block, $y_n^{(f_D)}$, will be the sum of the time-domain blocks associated to the N_R sets of rays, as follows by

$$y_n^{(f_D)} = \sum_{r=1}^{N_R} y_n^{(r)} e^{j2\pi f_D^{(r)} n/N}, \tag{32}$$

where $f_D^{(r)}$ denotes the Doppler drift associated to the rth cluster of rays. Let

$$\theta_n^{(r)} = 2\pi f_D^{(r)} \frac{n}{N}, \tag{33}$$

then (32) can be rewritten as

$$y_n^{(f_D)} = \sum_{r=1}^{N_R} y_n^{(r)} e^{j\theta_n^{(r)}}. \tag{34}$$

Under these conditions the transmitter chain associated to each one of the N_R cluster of rays can modeled as shown in the left side of Fig. 6. Considering a transmission associated to the rth cluster of rays, in the presence of a Doppler drift $f_D^{(r)}$, then the block of time-domain data symbols is affected by a phase rotation (before the channel), resulting in the

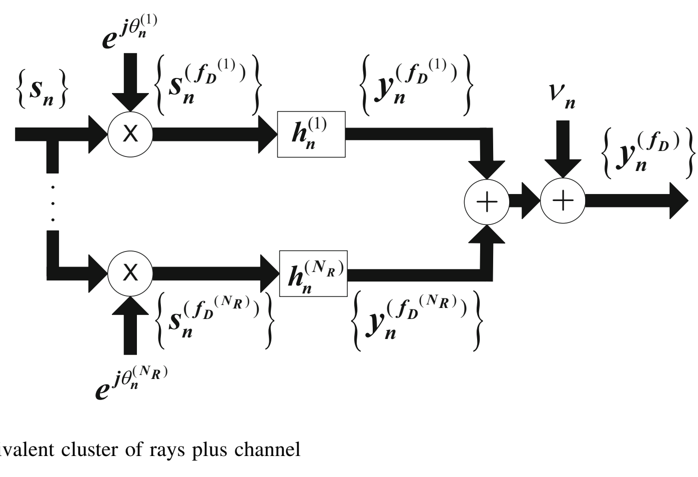

Fig. 6 Equivalent cluster of rays plus channel

effectively transmitted block, $\{s_n^{(f_D^{(r)})}; n = 0, \ldots, N-1\}$. It follows from (34) that the Doppler drift induces a rotation $\theta_n^{(r)}$ in the block's symbols that grows linearly along the time-domain block. Obviously, the effect of this progressive phase rotation might lead to a significant performance degradation.

In the following we propose two frequency domain receivers, based on the IB-DFE, with joint equalization and Doppler drift compensation. The first receiver whose structure is depicted in Fig. 7 has small modifications compared to the IB-DFE, and employs joint equalization and Doppler drift compensation.It considers the equivalent channel, in which the received signals associated to the N_R sets of rays are added leading to the signal $y_n^{(f_D)}$. To perform the Doppler drift compensation, we could employ a simple method based on the fact that the equivalent frequency drift, $\hat{f}_D$, corresponds to the one (previously estimated) associated to the strongest sub-channel. However, each sub-channel can be associated to a different phase rotation, so an average phase compensation is more appropriate. Thus, for this iteration, the Doppler drift compensation technique is based on a weighted arithmetic mean, in order to combine average values from samples corresponding to the frequency drifts associated to the different sub-channels. The average power associated to each sub-channel is denoted by

$$P^{(r)} = \sum_{n=0}^{N-1} |h_n^{(r)}|^2 = \frac{1}{N}\sum_{k=0}^{N-1} |H_k^{(r)}|^2, \tag{35}$$

and it is easy to see that the strongest sub-channel will have a higher contribution on the equivalent frequency drift. As result, the estimated frequency offset value and the estimated phase rotation are given by

$$\hat{f}_D = \frac{\sum_{r=1}^{N_R} P^{(r)} f_D^{(r)}}{\sum_{r'=1}^{N_R} P^{(r')}}, \tag{36}$$

and

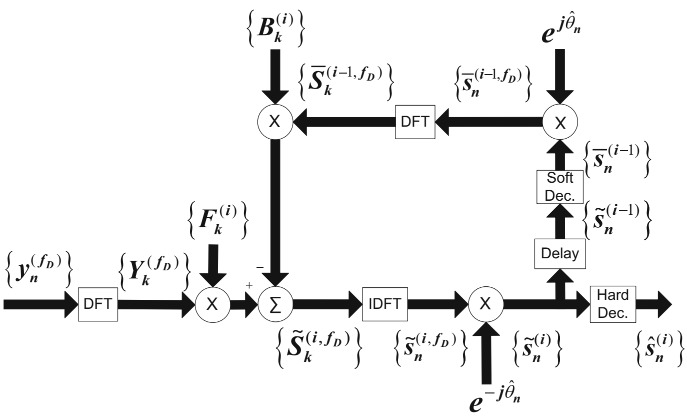

Fig. 7 Receiver structure for ADC

$$\hat{\theta}_n = 2\pi \hat{f}_D \frac{n}{N}, \tag{37}$$

respectively. After the compensation of the estimated phase rotation affecting the received signal, the resulting samples are passed through a feedback operation in order to complete the equalization procedures. The Doppler drift compensation technique employed in this receiver can be called as average Doppler compensation (ADC). However, the fact that it is based on an average phase compensation, might have implications in what refers to performance.

Let us consider now the second receiver shown in Fig. 8. This receiver employs a Doppler drift compensation technique called total Doppler compensation (TDC), which compensates the Doppler drift associated to each cluster of rays individually. It is worth mentioning that for the first iteration the process is equivalent to a linear receiver due to the absence of data estimates. Only for the subsequent iterations, this receiver will jointly compensate the Doppler drift and equalize the received signal. Hence, the feedback operations which will be described next are only valid for the subsequent iterations.

Let us consider the received signal referring to the rth cluster of rays, given by

$$\begin{aligned} y_n^{(f_D^{(r)})} &= y_n^{(f_D)} - \sum_{r' \neq r}^{N_R} y_n^{(f_D^{(r')})} = y_n^{(f_D)} - \sum_{r' \neq r}^{N_R} s_n^{(f_D^{(r')})} * h_n^{(r')} \\ &\approx y_n^{(f_D)} - \sum_{r' \neq r}^{N_R} \hat{s}_n e^{j\hat{\theta}_n^{(r')}} * h_n^{(r')} \approx y_n^{(f_D)} - \sum_{r' \neq r}^{N_R} \hat{y}_n^{(f_D^{(r')})}, \end{aligned} \tag{38}$$

where $*$ denotes the convolution operation. (The set of operations described next are performed for all N_R signals within each iteration). The first operation consists in isolating from the total received signal $y_n^{(f_D)}$ the signal associated to the r^{th} cluster of rays $y_n^{(f_D^{(r)})}$, which is accomplished by removing the contributions of the interfering signals as described in (38). The computation of the undesired signal components is based on the data estimates at the FDE's output from the previous iteration, $\{\hat{S}_k^{(i-1)}; k = 0, 1, \ldots, N-1\}$.

The samples corresponding to the resulting signal $\{y_n^{(f_D^{(r)})}; n = 0, \ldots, N-1\}$ are then passed to the frequency-domain by an N-point DFT, leading to the corresponding

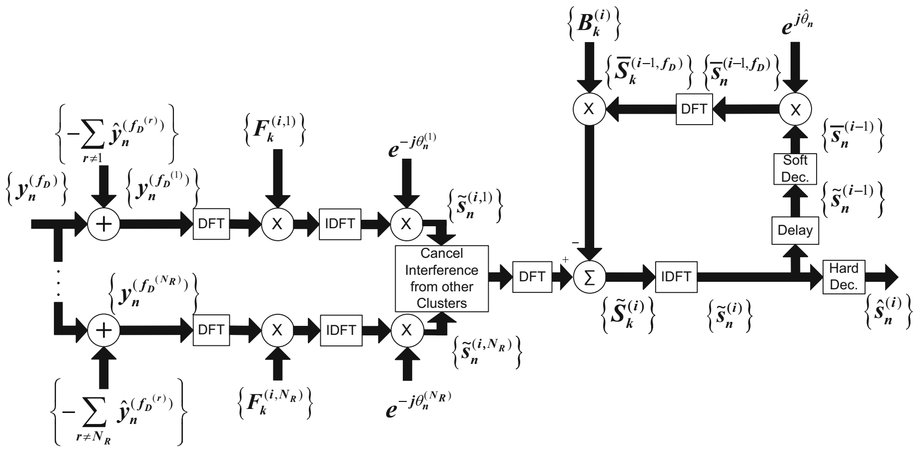

Fig. 8 Receiver structure for TDC

frequency-domain samples which are then equalized by a frequency-domain feedforward filter. The equalized samples are converted back to the time-domain by an IDFT operation leading to the block of time-domain equalized samples $\tilde{s}_n^{(f_D^{(r)})}$. Next, the resulting signal is compensated by the respective frequency drift $\theta_n^{(r)}$, which for simplicity it is assumed to have been previously estimated. This process is performed for each one of the clusters of multipath components, and the signals are added in a single signal which is then equalized with resort to the IB-DFE. The equalized samples at the FDE's output, will be given by $\{\hat{S}_k^{(i)}; k = 0, 1, \ldots, N-1\}$. Therefore, the receiver jointly compensates the phase error and equalizes the received signal by a Doppler drift compensation before the equalization and detection procedures.

5 Performance Results

Here we present a set of performance results regarding the use of the proposed receiver in time-varying channels.

We consider an SC-FDE modulation with blocks of $N = 1024$ symbols and a cyclic prefix of 256 symbols acquired from each block (although similar results were observed for other values of N, provided that $N \gg 1$). The modulation symbols belong to a QPSK constellation and are selected from the transmitted data according to a Gray mapping rule. We assumed linear power amplification at the transmitter. Our performance results are expressed as function of E_b/N_0, where N_0 is the one-sided power spectral density of the noise and E_b is the energy of the transmitted bits.

For each multipath group, the Doppler drift and the respective channel impulse response are obtained with the help of the frame structure presented previously in Sect. 3.1.

Firstly we consider the scenario from Fig. 9 where the receiver and all reflecting surfaces are fixed, and the transmitter (i.e., mobile terminal) is moving with speed v. It is also assumed a channel with uncorrelated Rayleigh fading, with multipath propagation, and with short-term variations due to Doppler effects. The maximum normalized Doppler drift is given by $f_d = f_D T_B = v f_c / c T_B$, with f_c denoting the carrier frequency, c the speed of light and T_B the block duration.

Let us consider now a critical scenario, where the multipath components are divided in two multipath clusters. The first cluster has the direction of movement and therefore is associated to a Doppler drift of $f_D^{(1)} = f_d$, while the second group has the opposite direction and a Doppler drift of $f_D^{(2)} = -f_d$. Without loss of generality we will assume that 64 multipath components are arriving from each direction. We also consider a difference of 10 dBs between the powers of both clusters [with $(P^{(1)} > P^{(2)})$]. Figures 10 and 11 present the BER performance for the proposed methods where ADC and TDC are denoted as method I and method II, respectively, regarding a transmission with a maximum normalized Doppler drifts of $f_d = 0.05$ and

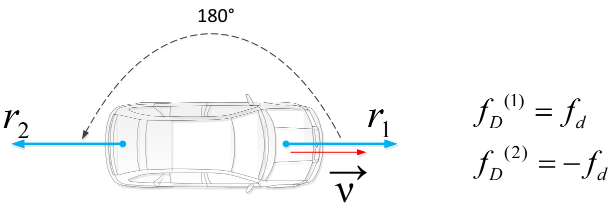

Fig. 9 Transmission scenario with two clusters of rays

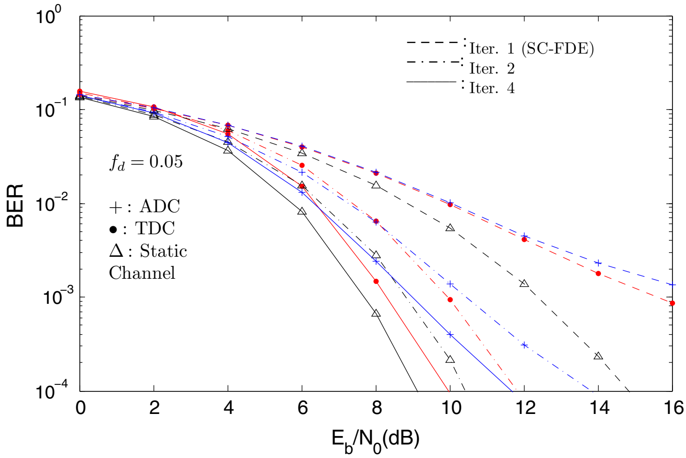

Fig. 10 BER performance for a scenario with normalized Doppler drifts f_d and $-f_d$ for $f_d = 0.05$

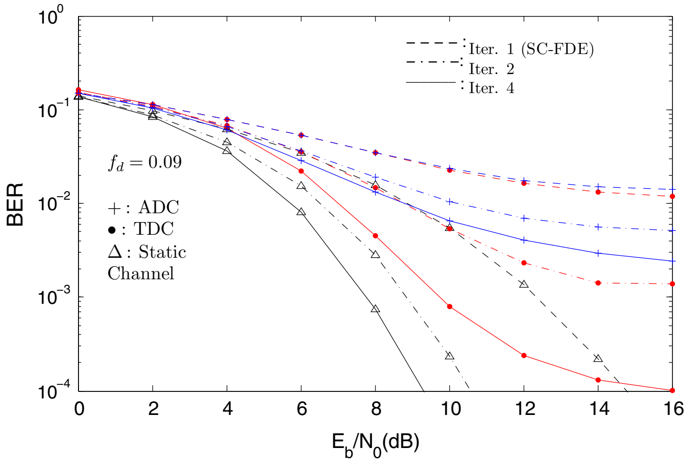

Fig. 11 BER performance for a scenario with normalized Doppler drifts f_d and $-f_d$ for $f_d = 0.09$

$f_d = 0.09$. For comparison purposes we also include the results for a static channel. Regarding the results, both compensation methods ADC and TDC, together with the IB-DFE iterations, can achieve high power gains, even with strong values of Doppler drifts. The two methods' performance is almost the same for BER values higher than 10^{-2}. For both scenarios, their performance is amazingly good when compared with the SC-FDE without compensation (see results for one iteration). As we can see from Fig. 10 at BER of 10^{-3}, the performance of both methods outperforms the SC-FDE by more than 6 dB. In fact the proposed compensation methods can achieve higher power efficiency even in presence of several groups of rays with significant differences on Doppler drifts. We also see that the TDC method gives the best error performance at the expense of computational complexity. Despite being more complex, for moderate values of Doppler drifts ($f_d \approx 0.05$), it outperforms the ADC method by 1.75 dB at the bit-error rate (BER) of 10^{-4}. For higher values of Doppler drifts, i.e $f_d \approx 0.09$, the method

TDC overcomes method ADC (whose BER performance highly deteriorates), achieving a gain of several dBs over ADC method. For instance from Fig. 11, for the 4^{th} iteration at BER of 10^{-3} the power gain is near to 7 dB. Again, we see that the TDC method performs very well and provides a good tradeoff between the error performance and the decoding complexity when compared with the ADC method. Moreover, for moderate Doppler drifts it can be seen from Fig. 10 that the second method's performance is close to the static channel (with a power degradation lower than 1 dB). Therefore, and despite the increase complexity, the receiver based on the second method has excellent performance, even when the different clusters of multipath components have strong Doppler effects.

6 Conclusions

In this paper we considered the use of SC-FDE schemes in channels with strong Doppler effects, which can be different for different multipath components. We proposed iterative frequency-domain receivers that are able to compensate these Doppler effects at the cost of a slight increase in complexity when compared with the IB-DFE. From our performance results we may conclude that the proposed compensation methods can achieve high gains, even for several groups of rays with substantially different Doppler drifts. Therefore, the proposed receivers are suitable for SC-FDE transmission, and can have excellent performance in the presence of fast-varying channels.

Acknowledgments This work was partially supported by the FCT (Fundaçãoo para a Ciência e a Tecnologia) under projects PEst-OE/EEI/LA0008/2013, HETCOP, ADIN (PTDC/EEI-TEL/2990/2012), CoPWIN (PTDC/EEI-TEL/1417/2012) and grant SFRH/BD/77847/2011.

References

1. Sari, H., Karam, G., & Jean claude, I. (1994). An analysis of orthogonal frequency-division multiplexing for mobile radio applications. In *Proceedings of IEEE VTC'94*, (Vol. 3, pp. 1635–1639).
2. Proakis, J. (1995). *Digital communications*. New York: McGraw-Hill.
3. Benvenuto, N., Dinis, R., Falconer, D., & Tomasin, S. (2010). Single carrier modulation with non linear frequency domain equalization: An idea whose time has come—Again. In *Proceedings of IEEE, no. 1* (Vol. 98, pp. 69–96).
4. Benvenuto, N., & Tomasin, S. (2002) Block iterative DFE for single carrier modulation. *IEEE Electronic Letters, 39*(19), 1144–1145.
5. Dinis, R., Gusmão, A., & Esteves, N. (2003). On broadband block transmission over strongly frequency-selective fading channels. In *Wireless 2003*. Canada: Calgary.
6. Dinis, R., Kalbasi, R., Falconer, D., & Banihashemi, A. (2004). Iterative layered space-time receivers for single-carrier transmission over severe time-dispersive channels. *IEEE Communications Letters*, *8*(9), 579–581.
7. Tüchler, M., & Hagenauer, J. (2000). Turbo equalization using frequency domain equalizers. In *Allerton conference*, October 2000.
8. Tüchler, M., & Hagenauer, J. (2001). Linear time and frequency domain turbo equalization. In *IEEE VTC'01 (Fall)*, October 2001.
9. Benvenuto, N., & Tomasin, S. (2005). Iterative design and detection of a DFE in the frequency domain. *IEEE Transactions on Communications*, *53*(11), 1867–1875.
10. Gusmão, A., Torres, P., Dinis, R., & Esteves, N. (2007). A turbo FDE technique for reduced-CP SC-based block transmission systems. *IEEE Transactions on Communications*, *55*(1), 16–20.
11. Sabbaghian, M., & Falconer, D. (2008). Joint turbo frequency domain equalization and carrier synchronization. *IEEE Transactions on Communications*, *7*(11), 204–212.
12. Dinis, R., Araújo, T., Pedrosa, P., & Nunes, F. (2010). Joint turbo equalisation and carrier synchronisation for SC-FDE schemes. *IEEE European Transactions on Telecommunications*, *21*(2), 131–141.
13. Rappaport, T. (2001). *Wireless communications: Principles and practice*. New Jersey: Wireless Communications: Principles and Practice.

14. Dent, P., Bottomley, G., & Croft, T. (1993). Jakes fading model revisited. *Electronics Letters*, *29*, 1162–1163.
15. Coelho, F., Dinis, R., & Montezuma, P. (2011). Efficient channel estimation for single frequency broadcast systems. In *IEEE VTC'11*, pp. 1–6, September 2011.

Fábio Silva received the M.S. degree from Faculdade de Ciências e Tecnologia, Universidade Nova de Lisboa, Portugal in 2010. Currently a scientific researcher, at the Instituto de Telecomunicações, in the area of wireless communications and finishing a Ph.D. degree in Electrical and Computer Science Engineering (early 2014), at the Universidade Nova de Lisboa (UNL), Faculdade de Ciências e Tecnologia (FCT), Portugal. He currently works at ANACOM, the Portuguese regulator for communications and radio spectrum management. His main research interests include modulation, equalization, and channel coding.

Rui Dinis (S96-M00) received the Ph.D. degree from Instituto Superior Técnico (IST), Technical University of Lisbon, Lisbon, Portugal, in 2001. Since 2001 he has been a professor at IST. He was a member of the research centre CAPS/IST (Centro de Análise e Processamento de Sinais) from 1992 to 2001. Since 2002 he has been a member of the research centre ISR/IST (Institute for Systems and Robotics). He has been with the Department of Electrical Engineering (DEE) of FCT-UNL, since 2009. He has been involved in several research projects in the broadband wireless communications area. His main research interests include modulation, equalization, and channel coding.

Paulo Montezuma received the Ph.D. degree from Faculdade de Ciências e Tecnologia, Universidade Nova de Lisboa (FCTUNL), Portugal, in 2007. He has been with the Department of Electrical Engineering (DEE) of FCT-UNL, since 2001. He was a member of the research center CAPS/IST (Centro de Análise e Processamento de Sinais) from 1996 to 2005. Since 2001 he is a researcher at UNINOVA. He has been involved in several research projects in the communications area, both national and European. His main research interests include modulation, channel coding, signal design for satellite and spreadspectrum systems.